

Available at [www.sciencedirect.com](http://www.sciencedirect.com)journal homepage: [www.elsevier.com/locate/he](http://www.elsevier.com/locate/he)

# Generation of hydrogen from NADPH using an [FeFe] hydrogenase

Phillip R. Smith<sup>a,1</sup>, Alyssa S. Bingham<sup>a,2</sup>, James R. Swartz<sup>a,b,\*</sup>

<sup>a</sup>Department of Chemical Engineering, Stanford University, 381 North South Mall, Stauffer III, Room 113, Stanford, CA 94305-5025, USA

<sup>b</sup>Department of Bioengineering, Stanford University, 381 North South Mall, Stauffer III, Room 113, Stanford, CA 94305-5025, USA

## ARTICLE INFO

### Article history:

Received 7 December 2010

Received in revised form

22 March 2011

Accepted 29 March 2011

Available online 11 May 2011

### Keywords:

Biohydrogen

Hydrogenase

Synthetic enzyme pathway

Ferredoxin-NADPH-reductase

Ferredoxin

## ABSTRACT

Biological technologies for the renewable conversion of biomass to hydrogen, an important chemical feedstock and potential fuel, could reduce greenhouse gas emissions by displacing the current source of virtually all hydrogen: fossil fuels. However, current fermentative methodologies suffer from low productivities and conversion yields. Previous work has shown that purified enzymes from the pentose phosphate pathway can be used to efficiently transfer the reducing equivalents in glucose to NADPH; this approach used a [NiFe] hydrogenase to directly produce hydrogen from NADPH. However, [FeFe] hydrogenases offer much higher hydrogen production activities. We demonstrate a new enzymatic method for the conversion of NADPH reducing equivalents to hydrogen by first using ferredoxin-NADPH-reductase to transfer electrons from NADPH to ferredoxin. The reduced ferredoxin then delivers the electrons to a [FeFe] hydrogenase for hydrogen production. This alternative *in vitro* pathway enables utilization of the fastest known hydrogenases, [FeFe] hydrogenases, and activates electron delivery by the native electron donor for these hydrogenases, ferredoxin. We report proof-of-principle data for this synthetic enzyme pathway, showing high volumetric production rates and hydrogenase turnover numbers relative to previous results utilizing [NiFe] hydrogenases.

Copyright © 2011, Hydrogen Energy Publications, LLC. Published by Elsevier Ltd. All rights reserved.

## 1. Introduction

Hydrogen is an important chemical feedstock, mainly used in refineries for upgrading liquid fuels and in the Haber–Bosch process for ammonia synthesis [1]. It is also envisioned to play a major role as a fuel in a future hydrogen economy [2]. However, steam reforming of methane and other fossil fuels, which is used for virtually all of the world-wide hydrogen production [1,3], generates CO<sub>2</sub>, a byproduct implicated as a causative agent in global warming. Thus, hydrogen

production methods that are renewable and carbon-neutral could be highly beneficial.

Biomass has played an important role in energy production throughout human history, mostly through direct combustion to produce useful heat [4]. It is a renewable resource generated by carbon-fixing organisms from sunlight, water, and CO<sub>2</sub>. Given the tremendous annual global production of biomass [3], this resource has the potential to be part of a multifaceted solution to current energy challenges. New methods for converting biomass to useful fuels and chemicals have gained

\* Corresponding author. Department of Chemical Engineering, Stanford University, 381 North South Mall, Stauffer III, Room 113, Stanford, CA 94305-5025, USA. Tel.: +1 650 723 5398; fax: +1 650 725 0555.

E-mail addresses: [psmith2@stanford.edu](mailto:psmith2@stanford.edu) (P.R. Smith), [abingham@stanford.edu](mailto:abingham@stanford.edu) (A.S. Bingham), [jswartz@stanford.edu](mailto:jswartz@stanford.edu) (J.R. Swartz).

<sup>1</sup> Tel.: +1 650 724 4969; fax: +1 650 725 0555.

<sup>2</sup> Tel.: +1 650 723 0274; fax: +1 650 725 0555.

0360-3199/\$ – see front matter Copyright © 2011, Hydrogen Energy Publications, LLC. Published by Elsevier Ltd. All rights reserved.

doi:10.1016/j.ijhydene.2011.03.172

traction in recent years, but current production costs are not competitive with fossil fuels [5]. Despite this, research is ongoing to find more cost-effective routes to transform biomass to usable fuels and chemicals in a carbon-neutral manner. Converting biomass to hydrogen could provide a sustainable supply of hydrogen for fertilizer production and other purposes [1,3].

There are currently two general methodologies for transforming biomass to hydrogen: (1) thermochemical and (2) biochemical [3,5]. In the first, heat is used to breakdown biomass, producing a gas consisting of CO and H<sub>2</sub>. In the second, enzymes are used to break down biomass to its constituent sugar monomers and convert the electrons and protons in the sugar monomers to hydrogen via a series of enzymatic reactions, culminating with the hydrogenase-catalyzed conversion of two protons and two electrons to dihydrogen (H<sub>2</sub>).

The economical breakdown of biomass to its constituent sugars has been a technical barrier hindering the deployment of biochemical biomass to fuel processes [6,7]. Consequently, there has been tremendous effort over the last decades to develop more effective pretreatment methods as well as cellulases with enhanced functional properties [8–10]. As these new methods emerge, they can provide more economical saccharide feedstocks for a variety of biofuels, including hydrogen.

Two strategies for the enzymatic conversion of biomass sugars to hydrogen have been studied: (1) fermentation, wherein metabolically engineered microorganisms process the sugars and produce hydrogen, and (2) *in vitro* hydrogen production, using a synthetic enzymatic pathway to direct electrons to the hydrogenase for H<sub>2</sub> synthesis. The yields from fermentative biohydrogen processes are typically low (2–4 mol of H<sub>2</sub> per mole glucose) [1,3], as the microorganism has its own metabolic needs that must be satisfied, and fermentative byproducts such as acetate or ethanol also accumulate.

*In vitro* biohydrogen production can achieve higher yields because cellular metabolic needs are eliminated. Zhang et al. [11], extending previous work by Woodward et al. [12–14], achieved yields of 8.35 mol H<sub>2</sub> per mole glucose-6-phosphate (G6P) using a synthetic pathway consisting of thirteen purified enzymes from the pentose phosphate pathway (PPP) coupled with the [NiFe] hydrogenase from *Pyrococcus furiosus*. In this pathway, the PPP transferred reducing equivalents from G6P to NADP<sup>+</sup>, forming NADPH, which was then consumed by the hydrogenase to produce hydrogen. This yield is substantially closer to the theoretical maximum of 12 mol H<sub>2</sub> per mole glucose, but the initial rate of hydrogen production was only 0.75 mmol H<sub>2</sub> L<sup>−1</sup> h<sup>−1</sup>. This corresponds to an energy volumetric productivity of 0.2 kJ L<sup>−1</sup> h<sup>−1</sup> and is low compared to the 40 kJ L<sup>−1</sup> h<sup>−1</sup> productivities estimated for current US bioethanol processes. Also, the turnover number (TON) of the hydrogenase was 0.005 s<sup>−1</sup> in the Zhang et al. work, suggesting very large quantities of this complex enzyme would be required for large-scale application of this technology.

Thus, while higher conversion yields are achievable with current *in vitro* methodologies than with fermentative processes, industrial-scale application of either technology is still impractical due to low volumetric hydrogen productivities.

In addition, using multiple purified enzymes for a full-scale industrial process would most likely be prohibitively expensive. While these examples provide important preliminary information, they also highlight the limiting factors that must be overcome to provide an economical industrial-scale process for the biological production of hydrogen from biomass.

Hydrogenases are metalloproteins, containing complicated metal centers that catalyze the interconversion of protons and electrons with dihydrogen. There are two main classes: (1) [NiFe] and (2) [FeFe], designations that indicate the metal atoms that are coordinated in the active site. Both types of hydrogenases require multiple maturases to synthesize and install the active site; six proteins are required for the [NiFe] hydrogenases while three maturation proteins are required for the [FeFe] hydrogenases [15–17]. The [FeFe] hydrogenases are typically much more active hydrogen producers than the [NiFe] hydrogenases [18]. However, both types of hydrogenases are susceptible to deactivation by molecular oxygen. While some [NiFe] hydrogenases are less oxygen sensitive and can be partially reactivated after oxygen exposure [19–22], this is usually not the case with [FeFe] hydrogenases. They must be assembled, activated, stored, and used anaerobically to be functional. Further, the hydrogenases and maturases each require iron and sulfur for assembly of the Fe–S clusters in the proteins, which complicates production. Fortunately, our lab recently reported a high-yielding *Escherichia coli*-based method for overexpressing and purifying the [FeFe] hydrogenases from *Clostridium pasteurianum* and *Chlamydomonas reinhardtii* [23].

Still, given the complexity of the hydrogenases and their maturases and the challenges involved in their large-scale production, industrial hydrogen production will likely require efficient use of the hydrogenases to be economically feasible, i.e., high TONs. Developing a pathway that will support higher TONs is therefore a key objective, in addition to high volumetric productivity and efficient conversion.

In this paper we propose a new enzymatic pathway for the delivery of electrons to the [FeFe] hydrogenase from *C. pasteurianum* (CpI) for the production of hydrogen from NADPH (Fig. 1). This new pathway is designed to be coupled to the output of the PPP, NADPH, and thus could be easily extended for production of hydrogen from glucose and from five-carbon sugars typically associated with biomass, such as xylose. The other two major proteins utilized in the pathway shown in Fig. 1 include the single electron-carrying *Synechocystis*

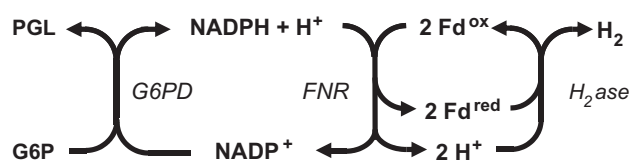


**Fig. 1 – Synthetic enzymatic pathway for hydrogen production from NADPH using purified enzymes.** Abbreviations: glucose-6-phosphate (G6P), glucose-6-phosphate dehydrogenase (G6PD), ferredoxin-NADPH-reductase (FNR), oxidized ferredoxin (Fd<sup>ox</sup>), reduced ferredoxin (Fd<sup>red</sup>), 6-phosphoglucono-δ-lactone (PGL), [FeFe] hydrogenase (H<sub>2</sub>ase). G6P and G6PD constitute a NADPH regeneration system used to maintain NADPH levels during hydrogen production.

[2Fe–2S] ferredoxin (SynFd), an iron sulfur protein that we have previously produced in our lab [24], and the *E. coli* ferredoxin-NADPH-reductase (FNR), which is a well-studied flavoprotein that catalyzes the transfer of electrons from NADPH to ferredoxin [25–28]. We describe the activation of this pathway and demonstrate a significant improvement in productivities and hydrogenase TONs relative to those previously reported for *in vitro* hydrogen production pathways. The pathway we present is also useful for studying [FeFe] hydrogenase reactivity and properties under conditions representative of the native electron delivery system [29].

## 2. Materials and methods

### 2.1. FNR cloning, overexpression, and purification

#### 2.1.1. Cloning

The gene for the *E. coli* FNR (*fpr*) was PCR amplified from the chromosome of *E. coli* strain BL21(DE3) using the primers 5'-CTTAAGCATATGGCTGATTGGGTAACAGGC-3' and 5'-CTA-TAGTCGACTTATTACCGTAATGCTCCGCTG-3' (the *SalI* and *NdeI* restriction sites are underlined). The PCR product was digested with *SalI* and *NdeI* (NEB, Boston, MA), and ligated into the pET21b expression vector (Novagen, San Diego, CA) with T4 ligase (NEB). The pET21b vector was digested with the same restriction enzymes for insertion between the T7 promoter and terminator. The ligation product was transformed into chemically competent DH5 $\alpha$  cells (Invitrogen, Carlsbad, CA) by heat shock at 42 °C. The resulting pET21bFNR vector was purified from 5 mL of culture using a QIAprep Spin Miniprep Kit (Qiagen, Valencia, CA) and retransformed into chemically competent BL21(DE3) cells (Invitrogen) by heat shock at 42 °C. The pET21bFNR sequence was confirmed by sequencing. Strains were maintained as frozen stocks in 25% glycerol.

#### 2.1.2. Overexpression

One liter of TB media (Invitrogen) with 100  $\mu$ g/mL ampicillin (Sigma–Aldrich) was inoculated with the BL21(DE3) pET21bFNR strain; the culture was grown at 30 °C in a 2L Tunair shake flask with shaking at 280 rpm. After the culture reached an OD<sub>595</sub> of 2, production of FNR was induced by adding 0.5 mM IPTG (Invitrogen). After 5 h of expression, the OD<sub>595</sub> had reached 10.4 and the cells were harvested, flash frozen, and stored at –80 °C overnight.

#### 2.1.3. Purification

The cells were thawed on ice and resuspended in 50 mL of 25 mM Tris pH8 containing one dissolved protease inhibitor tablet (Roche Molecular Biochemicals, Nutley, NJ). The cell suspension was lysed in a continuous homogenizer (Avestin Emulsiflex-C50, Ottawa, Ontario, Canada) by a single pass at 20,000 psig. The resulting lysate was incubated at 4 °C with Benzonase DNase (125 units/gm cell paste) and rLysozyme (5 kunits/gm cell paste) (Novagen) and clarified at 30,000 g for 30 min. The supernatant was diluted 3-fold and loaded at 2 mL/min onto a 50 mL column containing DEAE sepharose fast flow resin (GE Healthcare). A distinct yellow band appeared in the column and was stationary through a 1 column-volume (CV) wash with 25 mM Tris pH8 and 2 CVs

of the same buffer with 20 mM NaCl. A linear salt gradient from 20 to 300 mM NaCl over 90 min at 2 mL/min was used to elute the yellow band, which was confirmed to contain FNR by SDS-PAGE analysis and activity in the cytochrome c reduction assay (Section 2.3). A second chromatographic step combined the yellow fractions, diluted them 4-fold in 25 mM Bis-tris, 25 mM NaCl, pH5.5, and loaded them onto a 20 mL SP sepharose fast flow column (GE Healthcare) at 0.5 mL/min. A yellow band formed and was stationary through a 2 CV wash with loading buffer. A linear salt gradient from 25 to 500 mM NaCl at 0.5 mL/min over 120 min eluted the yellow band. The yellow fractions were confirmed to contain active FNR and combined. The FNR was then concentrated to 8.3 mg/mL, and the solution buffer changed to 25 mM Tris, 33 mM NaCl, pH8 in an Amicon Stirred-cell concentrator (Millipore Corp, Bedford, MA) using a 3 kDa MW-cutoff membrane. Glycerol was added to 5% and the FNR stored at –80 °C until use.

### 2.2. Ferredoxin cloning, overexpression and purification

The *Synechocystis* sp. PCC 6803 ferredoxin (SynFd) was produced in *E. coli* and purified with modifications to a previously reported method [24].

#### 2.2.1. Cloning

For *in vivo* expression, the *pefF* gene for the SynFd was removed from the pK7Fd vector [24] by digestion with *NdeI* and *SalI* and ligated into the pET21b expression vector with T4 ligase, which had been digested with the same enzymes to enable insertion between the T7 promoter and terminator. The ligated vector was transformed into chemically competent BL21(DE3) cells by heat shock at 42 °C; the pET21bSynFd sequence was confirmed by sequencing. The strain was stored at –80 °C in 25% glycerol.

#### 2.2.2. Overexpression

Using a 10L Biostat B Fermentor (B Braun Biotech International, Allentown, PA), 9.5L of TB media was inoculated with 250 mL of a log-phase BL21(DE3) pET21bSynFd culture and grown at 30 °C with 100  $\mu$ g/mL ampicillin. One hour before induction, 2 mM Ferrous Ammonium Citrate (Sigma–Aldrich, St. Louis, MI) and 2 mM Cysteine (Sigma–Aldrich) were added. At an OD<sub>595</sub> of 3.5, the culture was induced with 0.5 mM IPTG. After 5 h of expression, the OD<sub>595</sub> reached 6.5 and the cells were harvested, flash frozen, and stored at –80 °C overnight.

#### 2.2.3. Purification

The SynFd was purified as previously described [24] with the following modifications: before clarification the lysate was incubated with Benzonase DNase (125 units/gm cell paste) and rLysozyme (5 kunits/gm cell paste) at 4 °C. Ammonium sulfate precipitation was first performed using ammonium sulfate at 50% of saturation. The supernatant was subjected to anion exchange chromatography as previously described. After combining the pink-colored fractions from anion exchange chromatography, the SynFd was concentrated to 12.2 mg/mL and buffer exchanged into 150 mM Tris pH7.4, 50 mM NaCl, in an Amicon Stirred-cell concentrator (Millipore Corp.) using a 1 kDa MW-cutoff membrane. Sucrose was added to a final concentration of 20% and the SynFd was stored at –80 °C until use.

### 2.3. Cytochrome C reduction assay

The presence of active FNR in the chromatography elution fractions and final formulated product was verified using the cytochrome c reduction assay [30,31] in a VERSamax Tunable Microplate Reader (Molecular Devices Corp., Sunnyvale, CA), located in an anaerobic glovebox (Coy Laboratories, Grass Lake, MI). Horse heart cytochrome c (Sigma–Aldrich) was used as the terminal electron acceptor following SynFd reduction by FNR, with NADPH (Sigma–Aldrich) as the electron source. The assay was monitored at 550 nm with each reagent present at saturating conditions (30  $\mu\text{M}$  SynFd and 50  $\mu\text{M}$  cytochrome c) in 100 mM Tris pH7. NADPH was added to a final concentration of 500  $\mu\text{M}$  to initiate the reaction. 1 mM G6P (Sigma–Aldrich) and 1 unit of yeast G6P dehydrogenase (G6PD, Sigma–Aldrich) were included to maintain a constant supply of NADPH.

### 2.4. Hydrogenase overexpression and purification

The *C. pasteurianum* hydrogenase I (CpI) used in these experiments was anaerobically overexpressed, purified, and stored as described previously [23].

### 2.5. Hydrogen production assay

Hydrogen production reactions were conducted using 100  $\mu\text{L}$  reaction volumes added to 250  $\mu\text{L}$  wells installed inside of 8.5 mL glass vials. All reaction mixtures were prepared inside an anaerobic glovebox with a 2% hydrogen, 98% nitrogen atmosphere. The following were first added to each vial: (1) *E. coli* FNR, (2) SynFd, (3) CpI, (4) 3 mM G6P, and (5) 5 units G6PD. The G6P and G6PD were added to regenerate NADPH during the reaction. The reaction solutions were buffered with 25 mM Tris pH7. The vials were then sealed with a septum and an aluminum crimp-cap, removed from the glovebox, and purged with nitrogen for 4 min to remove hydrogen from the headspace. Next, the vials were warmed to 37  $^{\circ}\text{C}$  in an incubator and then purged for an additional 4 min to remove any hydrogen formed by reduced FNR or SynFd delivering electrons to the hydrogenase prior to reaction initiation. The vial was next placed in a 37  $^{\circ}\text{C}$  water bath and the 100  $\mu\text{L}$  reaction mixture stirred at 225 rpm with a small stir bar. After temperature equilibration, NADPH was added to a final concentration of 7 mM to initiate the reaction. The hydrogen concentration in the headspace was measured by removing 200  $\mu\text{L}$  of the headspace gas with a glass syringe and injecting into an Agilent 6890 GC-TCD (Agilent Technologies, Palo Alto, CA), with a Shincarbon column (Restek, Corp., Bellefonte, PA). Between uses, the syringe needle was inserted into a vial containing 100%  $\text{N}_2$  to avoid oxygen contamination of the reaction headspace. No other gaseous species were detected by the GC analysis. Hydrogen concentrations were determined from peak areas by comparing to calibration curves from standards with known hydrogen concentrations. The volumetric hydrogen production rate ( $\text{mmole H}_2 \text{ L}^{-1} \text{ h}^{-1}$ ) was determined by dividing the rate of hydrogen production ( $\text{mmole H}_2 \text{ h}^{-1}$ ) by the liquid reaction volume. The CpI hydrogenase TON ( $\text{mmole H}_2 \text{ s}^{-1} \text{ mmol CpI}^{-1}$ , or  $\text{s}^{-1}$ ) was calculated by dividing the volumetric productivity by the CpI

hydrogenase concentration in the reactions. All reactions were performed in triplicate.

## 3. Results and discussion

The diagram in Fig. 1 illustrates a new enzymatic route for producing hydrogen from NADPH. This *in vitro* pathway is designed to integrate with the PPP, which, as demonstrated by Woodward and Zhang [11–14], can be used to produce NADPH from G6P at high-yields.

As shown in Fig. 1, FNR catalyzes the transfer of two electrons from NADPH to two single electron-carrying SynFd proteins. These two SynFd proteins subsequently deliver their electrons to the CpI hydrogenase, which catalyzes the conversion of the electrons and two protons to  $\text{H}_2$ . Also included is an NADPH regeneration system comprised of G6P and G6PD, which converts  $\text{NADP}^+$  to NADPH, generating 6-phosphoglucono- $\delta$ -lactone (PGL) and a free proton.

Initial calculations of rates of hydrogen production using the new pathway predicted that 2.6 nM CpI and 1.4  $\mu\text{M}$  FNR would catalyze a hydrogen productivity of 5  $\text{mmole H}_2 \text{ L}^{-1} \text{ h}^{-1}$ . This was based on experimentally determined turnover numbers for hydrogen production by the CpI hydrogenase from dithionite-reduced SynFd (534  $\text{s}^{-1}$ , data not shown) and SynFd reduction by FNR from NADPH (2  $\text{s}^{-1}$ , data not shown). Reactions attempted with these concentrations, however, produced no measurable hydrogen. We reasoned that higher concentrations of the pathway components might be needed since SynFd, the substrate for the two principle enzymes, is a macromolecule and would suffer from significantly slower diffusion rates relative to small molecular weight substrates. Increasing the concentration of each protein by 10-fold produced measurable rates of hydrogen production. Additional concentration increases and optimization of reaction conditions, described below, provided further improvement.

The time-course of a typical hydrogen production reaction is presented in Fig. 2. During the first 20 min of the reaction, the headspace hydrogen concentration increased linearly, allowing determination of the initial volumetric production

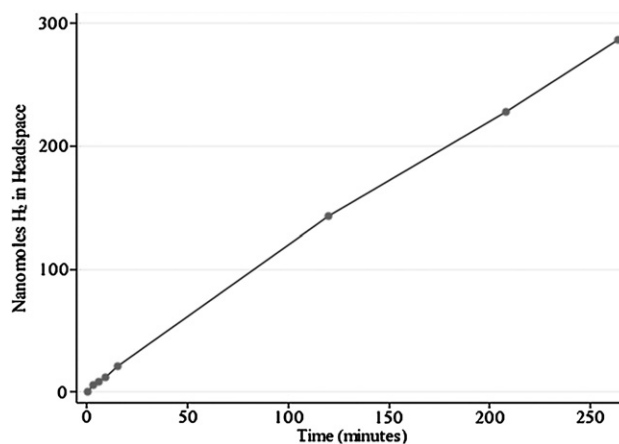


**Fig. 2 – Time-course of hydrogen production at 25  $^{\circ}\text{C}$ , with stirring. Protein concentrations were 1  $\mu\text{M}$  CpI, 30  $\mu\text{M}$  FNR, and 80  $\mu\text{M}$  SynFd.**



rate. Further data points highlight the sustained production of hydrogen over a period of several hours. Note that this is a batch reaction with significant hydrogen accumulation in contrast to the reactions reported previously, which used continuous gas purging to maintain very low hydrogen concentrations [11–14].

Fig. 3 shows the effects of optimizing the reaction temperature and reducing mass transfer limitations by stirring. Increasing the temperature from 25 to 37 °C more than tripled the volumetric hydrogen production rate (Fig. 3A). Additionally, stirring the reaction solution with a magnetic stir bar was also beneficial, as shown in Fig. 3B.

Fig. 4 shows the effects of changing the concentration of FNR, SynFd, and Cpl on the volumetric productivity and TON of the Cpl hydrogenase. For Fig. 4A, hydrogenase concentrations from 0.1 to 5  $\mu\text{M}$  were tested with 1  $\mu\text{M}$  Cpl giving the highest volumetric rate (3.5  $\text{mmol H}_2 \text{ L}^{-1} \text{ h}^{-1}$ ); higher TONs were obtained at the expense of lower volumetric productivity by decreasing the Cpl concentration to 0.1  $\mu\text{M}$ . In this case, the substantial increase in TON to 7  $\text{s}^{-1}$ , despite a moderate decrease in volumetric productivity, indicates that the hydrogenase is being utilized much more efficiently. However, this TON is still nearly two orders of magnitude less than the intrinsic Cpl TON as measured with dithionite-reduced SynFd (data not shown).

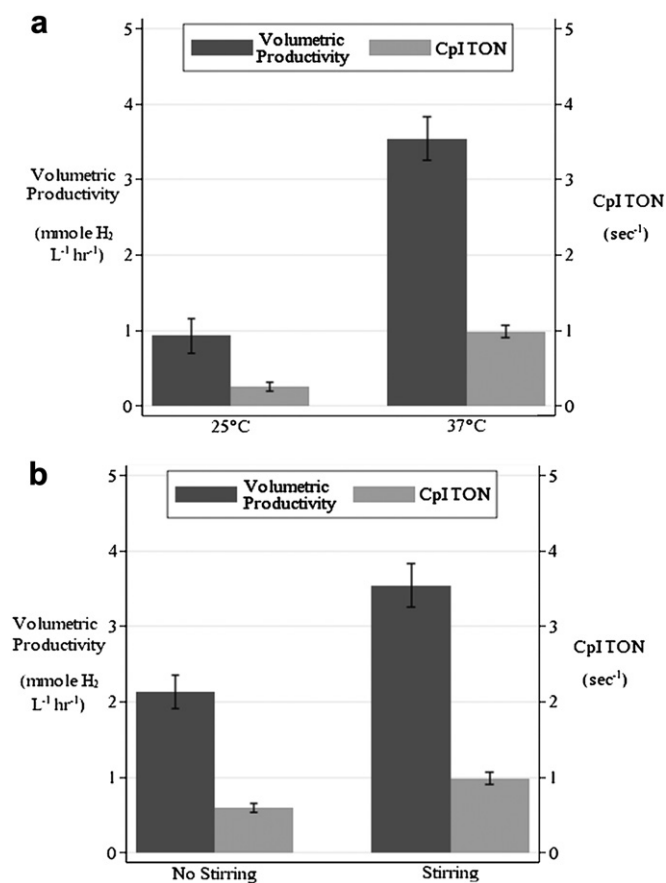


Fig. 3 – Effect of (A) temperature (with stirring) and (B) stirring (at 37 °C) on the rate of hydrogen production and the hydrogenase TON. Protein concentrations were 1  $\mu\text{M}$  Cpl, 30  $\mu\text{M}$  FNR, and 80  $\mu\text{M}$  SynFd.

The concentration of FNR was increased from 10 to 50  $\mu\text{M}$  and the volumetric rate improved to 4  $\text{mmol H}_2 \text{ L}^{-1} \text{ h}^{-1}$  (Fig. 4B). As shown in Fig. 4C, increasing the concentration of SynFd from 10 to 160  $\mu\text{M}$  significantly increased volumetric productivities and Cpl TONs; the highest observed rate was 5.7  $\text{mmol H}_2 \text{ L}^{-1} \text{ h}^{-1}$ , equivalent to a fuel-value productivity

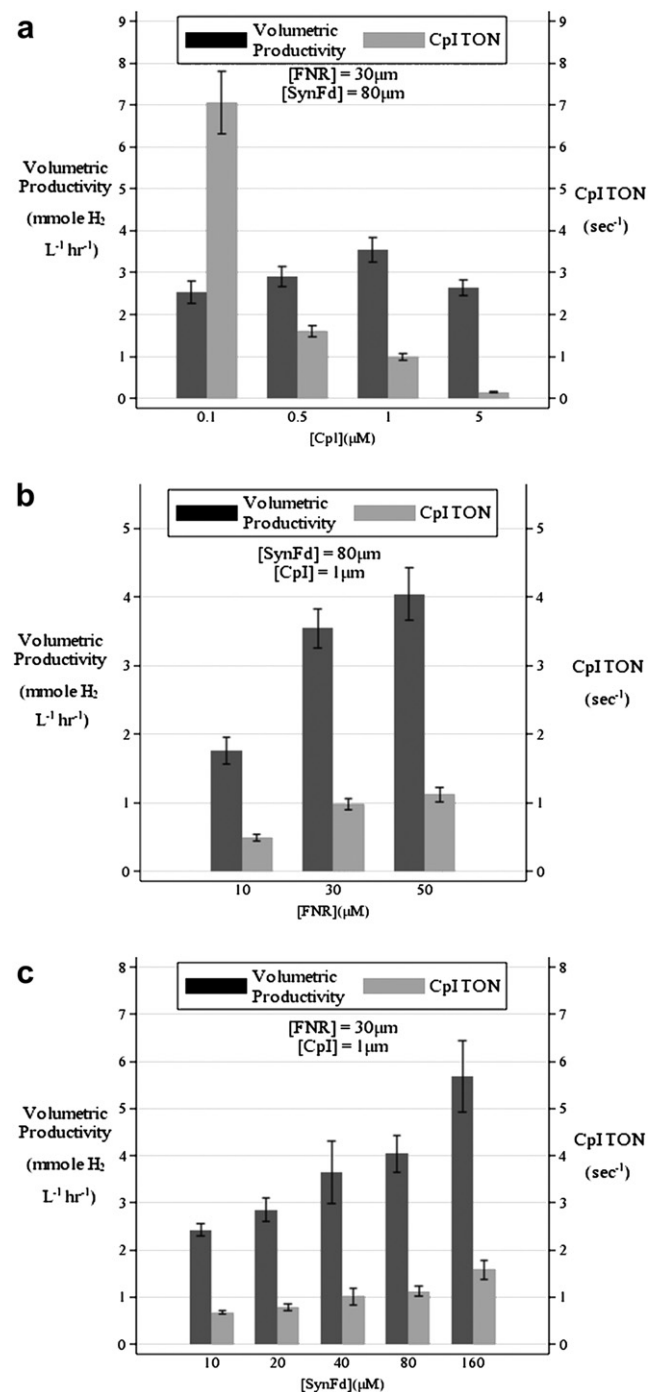


Fig. 4 – Effect of protein concentration on the rate of hydrogen production and on the Cpl hydrogenase TON. Protein concentrations (unless otherwise indicated) were 1  $\mu\text{M}$  Cpl, 30  $\mu\text{M}$  FNR, and 80  $\mu\text{M}$  SynFd. (A) Effect of varying [Cpl]; (B) Effect of varying [FNR]; (C) Effect of varying [SynFd].

of  $1.6 \text{ kJ L}^{-1} \text{ h}^{-1}$ . The concentration of available SynFd is an influential parameter as the protein must interact with both FNR and Cpl.

These experimental results indicate that the new enzyme pathway (Fig. 1) is a feasible and potentially attractive method for hydrogen production from NADPH. Initial experiments have substantially increased the volumetric production rates and the Cpl TONs. The reaction rates demonstrated through this pathway, in batch reaction mode, are an order of magnitude higher than those shown in previous work [11], and did not require the use of high gas purge rates. Further, hydrogen concentrations in the headspace approaching 1% were observed (data not shown), suggesting that thermodynamic limitations may not be a serious concern. As hydrogen separation and compression costs are important considerations in industrial hydrogen production, the ability to accumulate hydrogen to higher levels will be beneficial. As shown by the relatively low TONs of the Cpl hydrogenase reported in Figs. 2, 3 and 4, there is still significant room for improvement in the volumetric hydrogen production rate. Nonetheless, these proof-of-principle results strongly suggest the future commercial feasibility of this new reaction system.

#### 4. Conclusions

Biological production of hydrogen from biomass is a potentially attractive renewable and carbon-neutral source of an important chemical feedstock and potential fuel. We have proposed a method that leverages new technology for the conversion of cellulosic biomass to component sugars and subsequently to NADPH by providing a general route for the conversion of NADPH to hydrogen. This pathway is the first to employ an [FeFe] hydrogenase and the first to provide a mechanism for electron delivery by ferredoxin. We have presented data demonstrating hydrogenase TONs and hydrogen volumetric productivities that are an order of magnitude higher than for previous *in vitro* hydrogen production. This advance can now be combined with new and more effective heterologous hydrogenase production technologies [23], and can also be used as a tool to study hydrogenase functional characteristics [29].

Hydrogen production data obtained from changing the concentrations of each of the 3 major proteins in this pathway suggested that FNR and ferredoxin are currently limiting in the system. The highest volumetric productivity observed was  $5.7 \text{ mmole H}_2 \text{ L}^{-1} \text{ h}^{-1}$  and, under different conditions, the highest Cpl TON observed was  $7 \text{ s}^{-1}$ . These experiments improved the volumetric rates and hydrogenase TON, but the discrepancy between the observed TON ( $7 \text{ s}^{-1}$ ) and that produced with dithionite reduction of SynFd ( $534 \text{ s}^{-1}$ ) indicates substantial room for improvement.

We are pursuing several other options for improving the volumetric hydrogen production rate and TONs, including: (1) using the native ferredoxin for the Cpl hydrogenase, which is a two electron carrier, (2) testing intrinsically faster FNRs from different organisms, (3) optimizing reaction conditions (ionic strength, pH, etc) to facilitate better protein–protein interactions, and (4) developing measures to improve gas/liquid and liquid phase mass transfer rates. Given the intrinsic turnover

number of the Cpl hydrogenase, and the recent report from our lab of high-yield, heterologous overexpression of this fast enzyme [23], we expect future work to achieve energy productivities approximately an order of magnitude higher than current US bioethanol productivities.

#### Acknowledgments

The authors thank Sylvie Liong for assistance with hydrogen production experiments and Nicole T. Smith for assistance with figure preparation. This work was supported by the Global Climate and Energy Project at Stanford University (SPO #44473).

#### REFERENCES

- [1] Lee H-S, Vermaas WJF, Rittmann BE. Biological hydrogen production: prospects and challenges. *Trends Biotechnol* 2010;28:262–71.
- [2] Meherkotay S, Das D. Biohydrogen as a renewable energy resource - prospects and potentials. *Int J Hydrogen Energy* 2008;33:258–63.
- [3] Balat H, Kurtay E. Hydrogen from biomass – Present scenario and future prospects. *Int J Hydrogen Energy* 2010;35:7416–26.
- [4] Balat M. Mechanisms of thermochemical biomass conversion processes. Part 3: reactions of liquefaction. *Energy Source A* 2008;30:649–59.
- [5] Bartels JR, Pate MB, Olson NK. An economic survey of hydrogen production from conventional and alternative energy sources. *Int J Hydrogen Energy* 2010;35:8371–84.
- [6] Lynd LR, Weimer PJ, van Zyl WH, Pretorius IS. Microbial cellulose utilization: fundamentals and biotechnology. *Microbiol Mol Biol Rev* 2002;66:506–77.
- [7] Sun Y, Cheng J. Hydrolysis of lignocellulosic materials for ethanol production: a review. *Bioresour Technol* 2002;83:1–11.
- [8] Girio FM, Fonseca C, Carvalho F, Duarte LC, Marques S, Bogel-Lukasik R. Hemicelluloses for fuel ethanol: a review. *Bioresour Technol* 2010;101:4775–800.
- [9] Carvalho F, Duarte LC, Girio FM. Hemicellulose biorefineries: a review on biomass pretreatments. *J Sci Ind Res* 2008;67:849–64.
- [10] Alvira P, Tomás-Pejó E, Ballesteros M, Negro MJ. Pretreatment technologies for an efficient bioethanol production process based on enzymatic hydrolysis: a review. *Bioresour Technol* 2010;101:4851–61.
- [11] Zhang YHP, Evans BR, Mielenz JR, Hopkins RC, Adams MWW. High-yield hydrogen production from starch and water by a synthetic enzymatic pathway. *PLoS ONE* 2007;2:e456.
- [12] Woodward J, Cordray KA, Edmonston RJ, Blanco-Rivera M, Mattingly SM, Evans BR. Enzymatic hydrogen production: conversion of renewable resources for energy production. *Energy Fuels* 2000;14:197–201.
- [13] Woodward J, Orr M. Enzymatic conversion of sucrose to hydrogen. *Biotechnol Prog* 1998;14:897–902.
- [14] Woodward J, Orr M, Cordray K, Greenbaum E. Biotechnology: enzymatic production of biohydrogen. *Nature* 2000;405:1014–5.
- [15] Böck A, King PW, Blokesch M, Posewitz MC. Maturation of hydrogenases. In: Robert KP, editor. *Advances in microbial physiology*. Academic Press; 2006. p. 1–225.
- [16] Casalo L, Rousset M. Maturation of the [NiFe] hydrogenases. *Trends Microbiol* 2001;9:228–37.

- [17] Nicolet Y, Fontecilla-Camps JC, Fontecave M. Maturation of [FeFe] hydrogenases: structures and mechanisms. *Int J Hydrogen Energy* 2010;35:10750–60.
- [18] Frey M. Hydrogenases: hydrogen-activating enzymes. *ChemBiochem* 2002;3:153–60.
- [19] Lenz O, Ludwig M, Schubert T, Burstel I, Ganskow S, Goris T, et al. H<sub>2</sub> conversion in the presence of O<sub>2</sub> as performed by the membrane-bound [NiFe] hydrogenase of *Ralstonia eutropha*. *ChemPhysChem* 2010;11:1107–19.
- [20] Pandelia ME, Fourmond V, Tron-Infossi P, Lojou E, Bertrand P, Leger C, et al. Membrane-bound hydrogenase I from the hyperthermophilic bacterium *Aquifex aeolicus*: enzyme activation, redox intermediates and oxygen tolerance. *J Am Chem Soc* 2010;132:6991–7004.
- [21] Saggiu M, Ludwig M, Friedrich B, Hildebrandt P, Bittl R, Lenzian F, et al. Impact of amino acid substitutions near the catalytic site on the spectral properties of an O<sub>2</sub>-tolerant membrane-bound [NiFe] hydrogenase. *ChemPhysChem* 2010;11:1215–24.
- [22] Infossi P, Lojou E, Chauvin J-P, Herbette G, Brugna M, Giudici-Orticoni M-T. *Aquifex aeolicus* membrane hydrogenase for hydrogen biooxidation: role of lipids and physiological partners in enzyme stability and activity. *Int J Hydrogen Energy* 2010;35:10778–89.
- [23] Kuchenreuther JM, Grady-Smith CS, Bingham AS, George SJ, Cramer SP, Swartz JR. High-yield expression of heterologous [FeFe] hydrogenases in *Escherichia coli*. *PLoS ONE* 2010;5:e15491.
- [24] Boyer ME, Wang C-W, Swartz JR. Simultaneous expression and maturation of the iron-sulfur protein ferredoxin in a cell-free system. *Biotechnol Bioeng* 2006;94:128–38.
- [25] Aliverti A, Pandini V, Pennati A, de Rosa M, Zanetti G. Structural and functional diversity of ferredoxin-NADP(+) reductases. *Arch Biochem Biophys* 2008;474:283–91.
- [26] Carrillo N, Ceccarelli EA. Open questions in ferredoxin-NADP(+) reductase catalytic mechanism. *Eur J Biochem* 2003;270:1900–15.
- [27] Jarrett JT, Wan JT. Thermal inactivation of reduced ferredoxin (flavodoxin): NADP(+) oxidoreductase from *Escherichia coli*. *FEBS Lett* 2002;529:237–42.
- [28] Wan JT, Jarrett JT. Electron acceptor specificity of ferredoxin (flavodoxin): NADP(+) oxidoreductase from *Escherichia coli*. *Arch Biochem Biophys* 2002;406:116–26.
- [29] Bingham AS, Smith PR, Swartz JR. Evolution of an [FeFe] hydrogenase with decreased oxygen sensitivity. *Int J Hydrogen Energy* 2012;37:2965–76.
- [30] Seo D, Okabe S, Yanase M, Kataoka K, Sakurai T. Studies of interaction of homo-dimeric ferredoxin-NAD(P)(+) oxidoreductases of *Bacillus subtilis* and *Rhodospseudomonas palustris*, that are closely related to thioredoxin reductases in amino acid sequence, with ferredoxins and pyridine nucleotide coenzymes. *BBA-Proteins Proteomics* 2009;1794:594–601.
- [31] Yeom J, Jeon CO, Madsen EL, Park W. *In vitro* and *In vivo* interactions of ferredoxin-NADP(+) reductases in *Pseudomonas putida*. *J Biochem* 2009;145:481–91.